TRANSNAV
http://www.transnav.eu
the International Journal
on Marine Navigation
and Safety of Sea Transportation
Volume 12
Number 2
June 2018
DOI: 10.12716/1001.12.02.11

Ship Course Following and Course Keeping in Restricted Waters Based on Model Predictive Control

H. Liu, N. Ma & X.C. Gu
Shanghai Jiao Tong University, Shanghai, China

ABSTRACT: Ship navigation safety in restricted water areas is of great concern to crew members, because ships sailing in close proximity to banks are significantly affected by the so-called ship-bank interaction. The purpose of this paper is to apply the optimal control theory to help helmsmen adjust ships' course and maintain the target course in restricted waters. To achieve this objective, the motion of a very large crude carrier (VLCC) close to a bank is modeled with the linear equations of manoeuvring and the influence of bank effect on the ship hydrodynamic force is considered in the model. State-space framework is cast in a Multiple-Input Multiple-Output (MIMO) system, where the offset-free model predictive control (MPC) is designed for course following and the linear quadratic regulator (LQR) is used for course keeping. Simulation results show that the control methods effectively work in ship course following and course keeping with varying ship-bank distances and water depths. The advantage of adopting speed variation as the second control input is obvious.

1 INTRODUCTION

Course following and keeping in restricted waters is usually for ship berthing to dock or avoiding certain obstacles like other ships or constructions (as shown in Figure 1) in the waterways. The problem involves not only the course plan, but also the course keeping performance in confronting the disturbance of the ship-bank interaction. When a ship moves in proximity to a bank, it will experience a suction force towards the bank and a yawing moment, which is called ship-bank interaction or bank effect. Many published studies presented the way to estimate the bank induced forces (Norrbin 1974, Ch'ng et al. 1993), and also pointed that the ship-bank interaction can be quite huge to influence the ship's course keeping ability as well as directional stability (Fujino 1968, Sano et al. 2014, Liu et al. 2016).

The under-actuated nature of the ship manoeuvring problems, namely with more variables to be controlled than the number of control actuators, makes the control problem quite challenging (Fossen 2003). Such problem has received a lot of attention from the control community. Pettersen & Nijmeijer (2001) provided a high-gain, local exponential tracking result. By applying a cascade approach, a global tracking result was obtained in Lefeber et al. (2003). Path following approach based on the line-of-sight method was proposed by Moreira et al (2007) and then presented in more researchers' works (Børhaug et al. 2008, Skjetne et al. 2011). However, the performance of control systems is limited by the constraints on the control inputs. The aforementioned works has not taken the limitations into account.

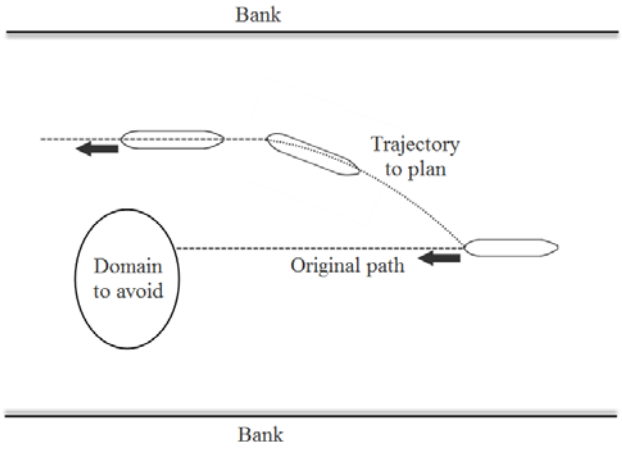

Figure 1. Trajectory control for avoidance in a waterway

The optimal control theory considering physical constraints was put forward to solve the problems of ship path planning (Djouani & Hamam 1995). Researches based on optimal theory have designed the ship path controller using methods like linear quadratic regulator (LQR) (Thomas & Sclavounos 2006, Mucha & el Moctar 2013) and evolutionary algorithms (Szłapczyński 2013). The model predictive control (MPC) approach, which allows multiple control inputs to response to the ship motion in the under-actuated system, has been used for path following (Oh & Sun 2009, Li et al. 2010), and improved with disturbance compensating unit to apply to ship heading control (Li & Sun 2012). A significant work by Feng et al. (2013) introduced the LQR to the MPC scheme to improve the robust control quality, so that the system can achieve the offset-free path following under external disturbances.

Enlightened by the previous work, this paper proposed a modified MPC scheme for the ship course following in close proximity to a bank, which combines the LQR to overcome the bank induced forces and maintain the ship course. The rationale of the MPC scheme aiming at course planning and the introduced unit of LQR for course keeping and system stabilization is elaborated in section 2. The illustration of bank induced forces and the corresponding hydrodynamic derivatives is given in section 3. In section 4, the performance of the controller is evaluated on the condition of different ship-bank distances, and the conclusion is drawn in the section 5.

2 NUMERICAL MODEL

2.1 *Maneuvering theory*

Figure 2 shows the coordinate systems as well as the variables used in the equations of ship motion. The earth-fixed coordinate system O_0-$\xi\eta\zeta$ and ship fixed coordinate system O-xyz are right-handed coordinate systems with the positive ζ and z axis pointing into the page and the origin O at the mid-ship point. The ship initially moves in the direction of the ξ axis with speed, U. Resulting from the bank effect, the ship's motion is defined as the vector [u, v, r], and the heading angle ψ as well as the drift angle β appears. δ denotes the rudder angle and y_{bank} denotes the ship-bank distance.

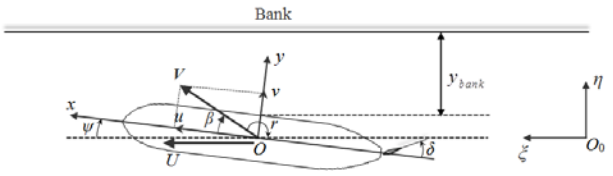

Figure 2. Coordinate systems

Small deviation in sway and yaw motion is caused by the rudder deflection and wind/bank forces. Therefore, the equation of surge motion is neglected and t the 2-DoF linear manoeuvring model of ship horizontal motion are given as:

$$\left(m+m_y\right)\dot{v}+\left(m+m_x\right)ur+mx_G\dot{r}=Y \tag{1}$$

$$\left(I_z+J_z\right)\dot{r}+mx_G\left(\dot{v}+ur\right)=N \tag{2}$$

where m is the ship mass and I_z is the yaw moment of inertia. m_x, m_y and J_z are the added mass and added moment of inertia for the surge, sway and yaw motion. Y and N represent the hydrodynamic sway force and yaw moment acting on the ship, which include hydrodynamic inertia terms and will be expressed by the following polynomial equations.

$$Y=Y_{\dot{r}}\dot{r}+Y_v v+Y_r r+Y_{\eta=0}+Y_\eta\eta+Y_\delta\delta \tag{3}$$

$$N=N_{\dot{v}}\dot{v}+N_v v+N_r r+N_{\eta=0}+N_\eta\eta+N_\delta\delta \tag{4}$$

Herein the force and moment caused by the bank effect are expressed as $Y_{\eta=0}+Y_\eta\eta$ and $N_{\eta=0}+N_\eta\eta$. The subscript "η=0" means the constant bank induced forces on the initial lateral position, and $Y_\eta\eta$ and $N_\eta\eta$ means the force due to the ship's lateral displacement η. The four items are called asymmetric derivatives.

All variables in the Equations 1 and 2 above are nondimensionalized in terms of ship length L, draft T, speed U and water density ρ through the equations as follows.

$$\begin{gathered}m'=\frac{m}{0.5\rho L^2T},\ I_z'=\frac{I_z}{0.5\rho L^4T},\ \dot{v}'=\frac{\dot{v}L}{U^2},\dot{r}'=\frac{\dot{r}L^2}{U^2}\\ u'=\frac{u}{U},\ v'=\frac{v}{U},\ r'=\frac{rL}{U},\ \eta'=\frac{\eta}{L},\ x_G'=\frac{x_G}{L}\\ Y'=\frac{Y}{0.5\rho LTU^2},\ N'=\frac{N}{0.5\rho L^2TU^2}\end{gathered} \tag{5}$$

Substituting Equations 3 and 4 into Equations 1 and 2, and nondimensionalizing the equations, the equations of ship manoeuvring is:

$$\mathbf{M}\begin{bmatrix}\dot{v}'\\ \dot{r}'\end{bmatrix}=\mathbf{N}\begin{bmatrix}v'\\ r'\end{bmatrix}+\mathbf{L}\left[\eta'\right]+\mathbf{F}_R\left[\delta\right]+\mathbf{F}_B \tag{6}$$

where

$$\mathbf{M}=\begin{bmatrix}-Y'_{\dot{v}}+m' & -Y'_{\dot{r}}+m'x'_G\\ -N'_{\dot{v}}+m'x'_G & -N'_{\dot{r}}+I'_z\end{bmatrix} \tag{7}$$

$$\mathbf{N}=\begin{bmatrix}-Y'_v & -Y'_r+m'\\ -N'_v & -N_r+m'x'_G\end{bmatrix} \tag{8}$$

$$\mathbf{L}=\begin{bmatrix}Y'_\eta\\ N'_\eta\end{bmatrix}\quad \mathbf{F}_R=\begin{bmatrix}Y'_\delta\\ N'_\delta\end{bmatrix}\quad \mathbf{F}_B=\begin{bmatrix}Y'_{\eta=0}\\ N'_{\eta=0}\end{bmatrix} \tag{9}$$

With variables v, r and η existing in (6), the heading angle ψ is added and the following expressions are deduced.

$$\begin{bmatrix}\dot{v}'\\ \dot{r}'\\ \dot{\psi}'\\ \dot{\eta}'\end{bmatrix}=\begin{bmatrix}-\mathbf{M}^{-1}\mathbf{N} & \begin{matrix}0\\0\end{matrix} & \mathbf{M}^{-1}\mathbf{L}\\ \begin{matrix}0&1\\1&0\end{matrix} & \begin{matrix}0&0\\1&0\end{matrix}\end{bmatrix}\begin{bmatrix}v'\\ r'\\ \psi\\ \eta'\end{bmatrix}+\mathbf{M}^{-1}\left(\mathbf{F}_R\left[\delta\right]+\mathbf{F}_B\right) \tag{10}$$

Since this dynamic system accepts a small scale variation of speed that is defined as Δu, the bank induced suction force and yaw moment in relation to forward speed can be expressed in the following form.

$$\begin{aligned}F_{bank}&=0.5\rho LdY'_{\eta=0}\left(U+\Delta u\right)^2\\&=0.5\rho LdY'_{\eta=0}\left(U^2+2U\Delta u+\Delta u^2\right)\end{aligned} \tag{11}$$

$$\begin{aligned}F_{bank}&=0.5\rho L^2dM'_{\eta=0}\left(U+\Delta u\right)^2\\&=0.5\rho L^2dM'_{\eta=0}\left(U^2+2U\Delta u+\Delta u^2\right)\end{aligned} \tag{12}$$

The last term in the equations above is of second order and negligible, while the second term directly shows the contribution of the perturbation velocity Δu to the bank induced forces. Keeping only leading order terms in the perturbation, the matrix of ship-bank hydrodynamics is rewritten as:

$$\begin{aligned}\mathbf{F}_B&=\begin{bmatrix}\dfrac{F_{bank}}{0.5\rho LdU^2}\\ \dfrac{M_{bank}}{0.5\rho L^2dU^2}\end{bmatrix}=\begin{bmatrix}Y'_{\eta=0}\\ N'_{\eta=0}\end{bmatrix}\cdot\left(\frac{U^2+2U\Delta u}{U^2}\right)\\&=\begin{bmatrix}Y'_{\eta=0}\\ N'_{\eta=0}\end{bmatrix}\left(1+2\Delta u'\right)\end{aligned} \tag{13}$$

Now the linearized manoeuvring model is put into the state equation with matrix form:

$$\dot{\mathbf{x}}=\mathbf{A}\mathbf{x}+\mathbf{B}\mathbf{u}+\mathbf{E} \tag{14}$$

where

$$\mathbf{x}=\left[v'\quad r'\quad \psi\quad \eta'\right]^T,\qquad \mathbf{u}=\left[\delta\quad \Delta u\right]^T \tag{15}$$

$$\mathbf{A}=\begin{bmatrix}-\mathbf{M}^{-1}\mathbf{N} & \mathbf{M}^{-1}\mathbf{L} & \begin{matrix}0\\0\end{matrix}\\ \begin{matrix}0&1\\1&0\end{matrix} & \begin{matrix}0&0\\0&1\end{matrix} & \end{bmatrix} \tag{16}$$

$$\mathbf{B}=\begin{bmatrix}\mathbf{M}^{-1}\left[\mathbf{F}_R & 2\mathbf{F}_B\right]\\ \begin{matrix}0&0\\0&0\end{matrix}\end{bmatrix},\quad \mathbf{E}=\begin{bmatrix}\mathbf{M}^{-1}\mathbf{F}_B\\ 0\\0\end{bmatrix} \tag{17}$$

2.2 *Course following control*

To simulate the course following process in the discrete-time scheme, the continuous-time model of Equation 14 is first discretized as:

$$\mathbf{x}_{k+1}=\mathbf{A}_d\mathbf{x}_k+\mathbf{B}_d\mathbf{u}_k+\mathbf{E}_d \tag{18}$$

The standard MPC scheme can be formulated based on the discrete model but unable to eliminate the steady cross-track error due to the existing disturbance of bank effect. So the MPC scheme proposed here is derived from the steady state system equations under the steady disturbance $\mathbf{E}_d$,

$$\begin{cases}\mathbf{x}_\infty=\mathbf{A}_d\mathbf{x}_\infty+\mathbf{B}_d\mathbf{u}_\infty+\mathbf{E}_d\\ \mathbf{y}_\infty=\mathbf{C}_d\mathbf{x}_\infty\end{cases} \tag{19}$$

where $\mathbf{u}_\infty$ is the steady state control; $\mathbf{y}_\infty$ is the output that is controlled to approach the desired value. Considering the following equation:

$$\mathbf{u}_\infty=-\left[\mathbf{C}_d\left(I-\mathbf{A}_d\right)^{-1}\mathbf{B}_d\right]^{-1}\mathbf{C}_d\left(I-\mathbf{A}_d\right)^{-1}\mathbf{E}_d \tag{20}$$

The current error dynamic formulation, in which $\mathbf{A}_d$ has two eigenvalues at 1, leads to a singular (I-$\mathbf{A}_d$) matrix. In this case the controller cannot give precise

response to balance the bank induced forces. To resolve this problem, the original system needs to be stabilized first through feedback while the MPC scheme determines the optimal control input at each time step. In this study, the stabilization is achieved by using LQR controller. The cost function and weighting matrices for the LQR controller are chosen to be the same as for the MPC. More specifically, the control input at each time step is divided into two parts:

$$\mathbf{u}_k = \mathbf{u}_k^{MPC} + \mathbf{u}_k^{LQR} = \mathbf{u}_k^{MPC} - \mathbf{K}_{LQR}\mathbf{x}_k \tag{21}$$

And the modified system dynamics will be:

$$\begin{aligned}\mathbf{x}_{k+1} &= \mathbf{A}_d\mathbf{x}_k + \mathbf{B}_d\left(\mathbf{u}_k^{MPC} - \mathbf{K}_{LQR}\mathbf{x}_k\right)\\ &= \left(\mathbf{A}_d - \mathbf{B}_d\mathbf{K}_{LQR}\right)\mathbf{x}_k + \mathbf{B}_d\mathbf{u}_k^{MPC} = \bar{\mathbf{A}}_d\mathbf{x}_k + \mathbf{B}_d\mathbf{u}_k^{MPC}\end{aligned} \tag{22}$$

With the stable system, the corresponding control input to overcome the ship-bank interaction forces can be calculated by:

$$\mathbf{u}_\infty^{MPC} = -\left[\mathbf{C}_d\left(I - \bar{\mathbf{A}}_d\right)^{-1}\mathbf{B}_d\right]^{-1}\mathbf{C}_d\left(I - \bar{\mathbf{A}}_d\right)^{-1}\mathbf{E}_d \tag{23}$$

It can be seen from Equation 22 and Equation 23 that the function of LQR includes: 1) to avoid the singular matrix (I- $\mathbf{A}_d$) as the system varies at each time step; 2) to stabilize the part of course keeping in the control system so that the MPC algorithm can be run in an offset-free situation.

As to the standard MPC scheme, first the cost function for minimization is:

$$\begin{aligned}J\left(\mathbf{U}_k^{MPC};\mathbf{x}_k\right) = \sum_{j=0}^{N_P-1}\Big[&\mathbf{x}_{k+j}^T\mathbf{Q}\mathbf{x}_{k+j} +\\ &\left(\mathbf{u}_{k+j}^{MPC} - \mathbf{u}_\infty^{MPC}\right)^T\mathbf{R}\left(\mathbf{u}_{k+j}^{MPC} - \mathbf{u}_\infty^{MPC}\right)\Big]\end{aligned} \tag{24}$$

$$\mathbf{U}_k^{MPC} = \left[\mathbf{u}_k^{MPC}, \mathbf{u}_{k+1}^{MPC}, \cdots, \mathbf{u}_{k+N_P-1}^{MPC}\right] \tag{25}$$

N_P is the prediction horizon; $\mathbf{Q}$ and $\mathbf{R}$ are the weighting matrices for the states and control inputs, respectively. $\mathbf{U}_k^{MPC}$ is the optimal control sequence, in which the $\mathbf{u}_k^{MPC}$ only is remained by the MPC scheme as the actual control input to be implemented. Notice that $\mathbf{u}_\infty^{MPC}$ is included in the cost function to achieve offset-free path following. The optimal control sequence is subject to:

$$-\mathbf{u}_{\max} - \mathbf{u}_{k+j}^{LQR} \le \mathbf{u}_{k+j}^{MPC} \le \mathbf{u}_{\max} - \mathbf{u}_{k+j}^{LQR} \tag{26}$$

$$\begin{cases}\mathbf{u}_{k+j-1}^{MPC} - \mathbf{u}_{k+j}^{LQR} \le \Delta\mathbf{u}_{\max}T_s + \left(\mathbf{u}_{k+j}^{LQR} - \mathbf{u}_{k+j-1}^{LQR}\right)\\ \mathbf{u}_{k+j}^{MPC} - \mathbf{u}_{k+j-1}^{LQR} \le \Delta\mathbf{u}_{\max}T_s - \left(\mathbf{u}_{k+j}^{LQR} - \mathbf{u}_{k+j-1}^{LQR}\right)\end{cases} \tag{27}$$

where j=0, 1 ,…,N_P; $\mathbf{u}_{\max}$ is the actuator constraint; $\Delta\mathbf{u}_{\max}$ is the constraints on the rate of actuator change; T_s is the sampling time.

3 ASYMMETRIC HYDRODYNAMIC FORCES

Table 1 lists the principal dimensions of the test model KVLCC2, which is a crude oil tanker as a benchmark for study of ship hydrodynamics. The PMM test was conducted in the CWC at Shanghai Jiao Tong University. The dimensions of measuring section are 8.0m×3.0m (water width) ×1.6m (water depth). In this experiment, the ship was placed laterally off the centerline of the CWC with different displacements η=0m-0.9m, corresponding to y_{bank}=2.8B-0.8B. The condition of water depth includes h=1.25T, h=1.5T and h=10.0T.

Table 1. Principle dimensions of the KVLCC2

Parameters		Full scale	Model
Length between perpendiculars	L m	320.00	2.4850
Breadth	B m	58.00	0.4504
Design draft	T m	20.80	0.1615
Displacement	Δ m^3	312540	0.1464
LCB from Mid-ship	xB m	11.04	0.086
Scale		128.77:1	

Figure 3 plots the nondimensional asymmetric force Y' and yaw moment N' versus lateral displacement in three water depths. As the sign of the values indicate, the ship experiences a suction force towards the bank and a bow-out moment turning the bow off the bank side. The forces increase as the ship moves to the bank, and the amplitudes of the forces soar as the water depth decreases. Each point is the value of $Y'_{\eta=0}$ or $N'_{\eta=0}$ at the corresponding position. The asymmetric derivatives Y'_η and N'_η are analyzed using the data surrounding the point. The asymmetric derivatives Y'_η and N'_η at y_{bank}=1.7B in the three water depths are presented in Table 2.

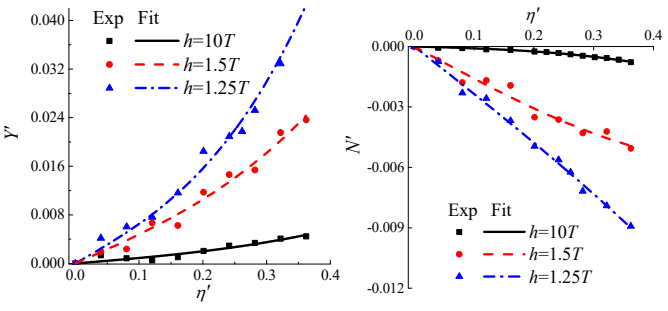

Figure 3. Asymmetric hydrodynamic forces versus η′ in different water depths.

Table 2. Asymmetric derivatives at y_{bank}=1.7B in three water depths

	h/T=1.25	h/T=1.5	h/T=10
Y'_η	0.0608	0.0463	0.0045
N'_η	-0.0235	-0.0161	-0.0007

4 SIMULATION OF COURSE CONTROL

The controller focuses on the trajectory following problem that is illustrated in Figure 1. Firstly the MPC scheme is tuned in the condition of h/L=0.5 where the bank effect can be ignored. The aim of the scheme is to make the ship proceed on a parallel course to the bank with a lateral distance of from the ship's initial course. The actuator constraints are $\mathbf{u}_{max}=[0.524\ 0.08]^T$ and $\Delta\mathbf{u}_{max}=[0.21\ 0.03]^T$; the sampling time Ts=1sec.

4.1 *Controller tuning*

The length of prediction horizon is first tuned by the simulations as shown in Figure 4. It reveals that the simulation results converge to the disired lateral value when N_P approaches to 20. And this achieves a good balance between the course control performance and the time consumption. So the length of prediction horizon is set as N_P =20 for further tuning of the weighting matrices.

The weighting matrices **Q** and **R** shape the closed loop response to achieve the desired performance in the form of **Q** ={0,0, q_1,q_2} and **R** ={r_1,r_2}. The tuning for the matrices is actually the trial-and-error program to find the optimum ratio between q_1 and q_2 as well as the ratio between r_1 and r_2.The ratio q_1/q_2 sets the preference for the controller to eliminate the cross-track errors while the ratio r_2/r_1 sets the preference for the controller to use one actuator over the other. Firstly q_1=10 and r_1=1, r_2=2 are selected while the value of q_2 is varied to examine the simulation results. As shown in Figure 5, the control scheme eliminates the cross-track error effectively with the range of q_1/q_2=1 to 10, but the path following performance deteriorate when q_1/q_2 reach 100. The amplitude of speed reduction also increases as the value of q_2 grows. Compared to the ratio q_1/q_2=10, the system succeeds in yielding a smaller fluctuation of the speed reduction during the whole process of the ship course adjustment and stabilization when q_1/q_2=1. So $q_1=q_2$=10 is chosen as the value of the **Q** matrix.

Finally, the tuning of r_2/r_1 is conducted by varying r_2 with the value of r_1 kept at 1. The results are presented in Figure 6. In the range from r_2/r_1=0.5 to r_2/r_1=10, the simulation results of ship trajectory and the rudder reflection do not change quite large, which proves the finding by Feng et al. (2013) that the **R** matrix has less influence on the course changing performance than the **Q** matrix. But too small r2 will put larger weight on the usage of ship speed change and cause the failure of the speed variation constraints. As the ship approaches to the desired path with the least overshoot rudder angle at the ratio r_2/r_1=2, the value r_1=1and r_2=2 is selected for the **R** matrix in the following simulations.

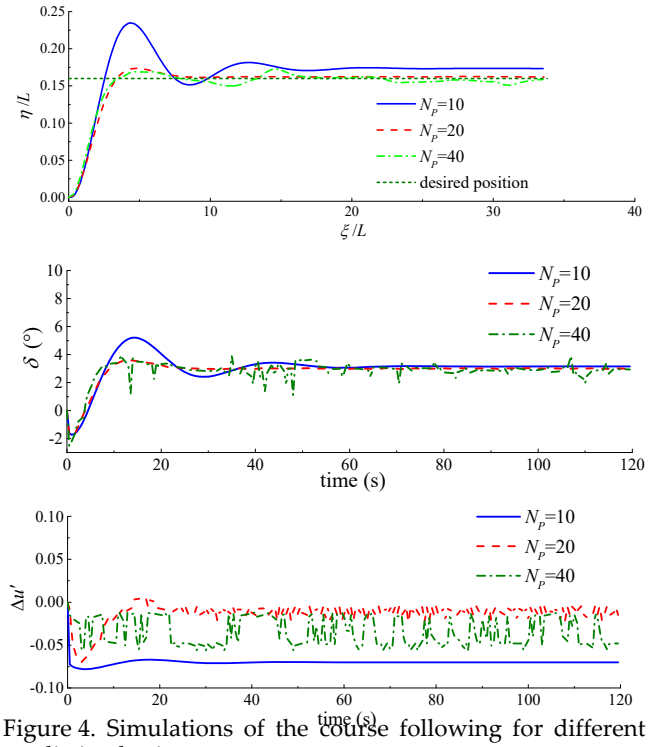

Figure 4. Simulations of the course following for different prediction horizons

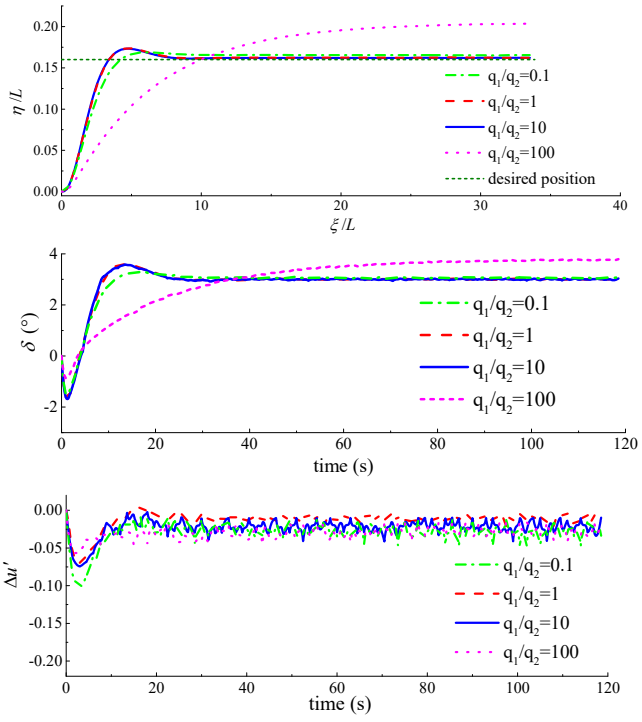

Figure 5. Simulations of the course following for different ratios between q_1 and q_2

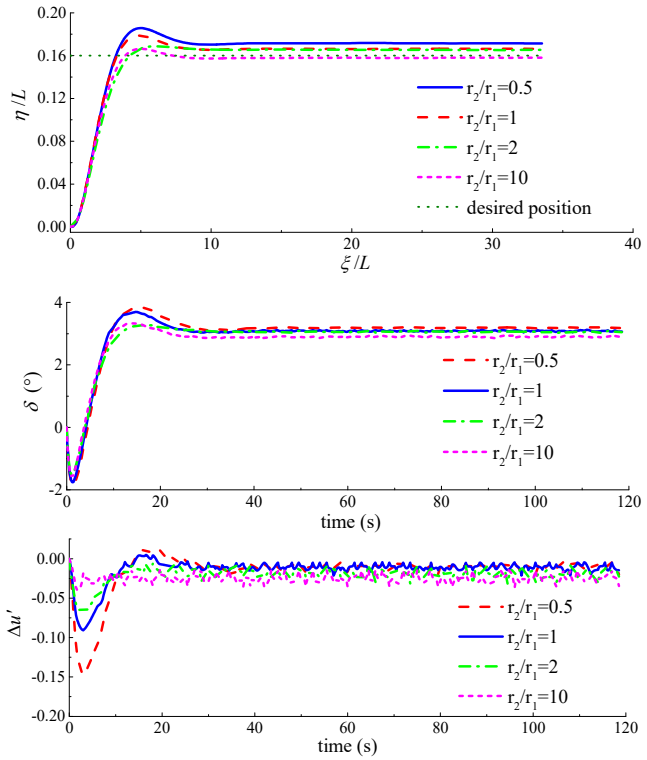

Figure 6. Simulations of the course following for different ratios between r1 and r2.

4.2 *Simulation in close proximity to banks*

The tuned scheme is further used for the course following of KVLCC2 ship from the initial course, which is y_{bank}=1.7B and y_{bank}=1.35B from the bank, to the target course that is 0.16L laterally from the initial course in the water depth of h=10T. The simulations are shown in Figure 7 and Figure 8, respectively. The combination of rudder deflection and speed variation as Multiple-Input Multiple-Output control (denoted as MIMO in the figures) is compared with the performance of rudder-control only (denoted as Rudder-only). The results show that the favourable prediction horizon and weighting matrices chosen for multiple input system also work for the single rudder case. The steady state error of η/L for two control schemes indicates that MIMO can eleminate the cross-track error more effectively than the scheme that uses the rudder only. This is because that the speed variation as the second input improves the course control performance. It is also noticeable that due to the offset-free scheme, there will be nonzero steady rudder angle as well as a certain value of speed reduction to overcome the bank induced forces.

Next, the effect of MIMO combined with offset-free MPC on course following and keeping is checked for different water depths, as presented in Figure 9. The initial course is located at y_{bank}=2.8B and the target course is 0.16L laterally from the initial course. The steady-state error in the lateral position becomes larger as the water depth decreases, owing to the rapidly increasing bank induced forces in shallow water. In the subplots of the control output, the amplitude of the rudder angle response significantly increases, and the speed reduction reaches the saturation point of $\Delta u'_{max}$=0.08, indicating that the demand of speed reduction is more than the upper limit of the actuator constraint. The possible way to eliminate steady-state errors is re-tuning the weighting matrix **Q** and **R** and turn up the limit of actuator constraint.

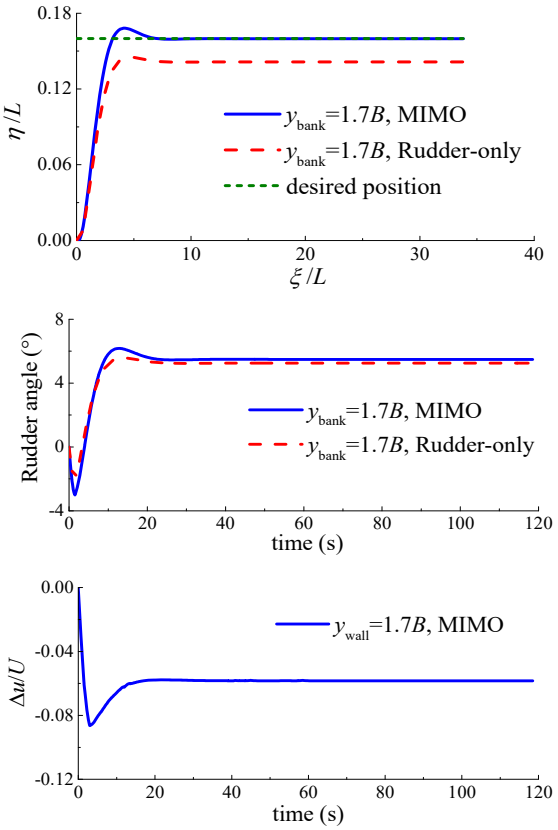

Figure 7. Simulations of the course following in close proximity to a bank (y_{bank}=1.7B)

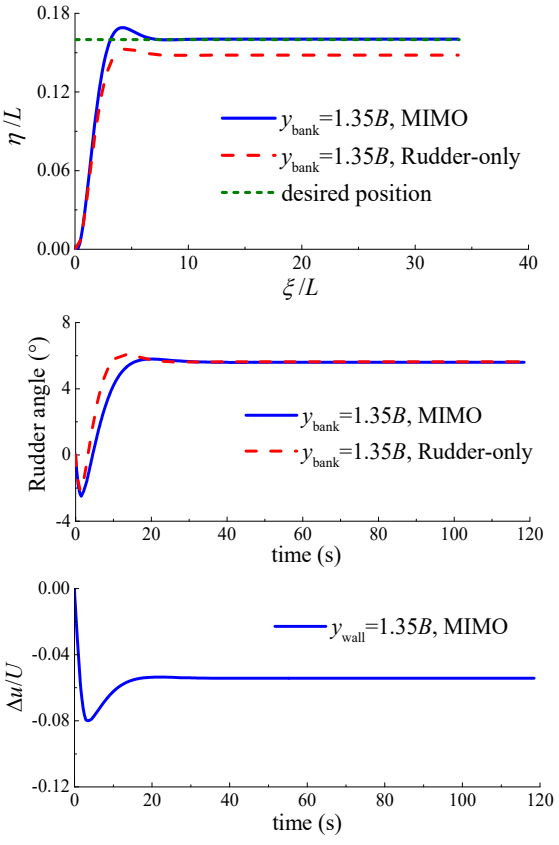

Figure 8. Simulations of the course following in close proximity to a bank (ybank=1.35B).

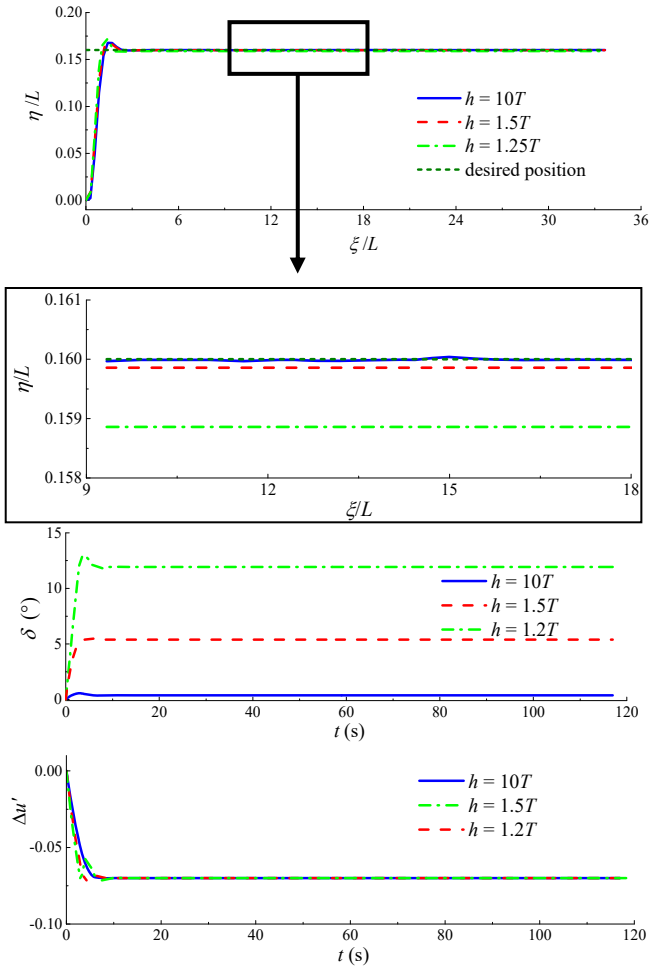

Figure 9. Simulations of the course following in different water depths.

5 CONCLUSIONS

The paper proposes the modified MPC scheme to solve ship course following in close proximity to the bank as well as counteracting bank effect. A linear manoeuvring model including the hydrodynamic components of bank induced forces is introduced and transformed to state equations for the design of control system. To stabilize the error dynamics formulation and to get a reliable solution of the control response to bank effect, the LQR unit is introduced into the system. And then the steady control input to overcome the disturbance due to bank effect is implemented into the MPC scheme. The controller is tuned first to obtain the suitable prediction horizon and weighting matrices for improving performance. Then, simulations of varying ship-bank distances are conducted. The feasibility of the offset-free MPC scheme in course following for ship proceeding close to a bank is proved. The advantage of adopting speed variation as the second control input is that the steady state errors under ship-bank interactions are reduced. In shallow waters, the steady-state error increases under the significantly enhancing ship-bank interaction. Therefore, the weighting matrix and the actuator constraint are suggested to be adjusted to provide higher control inputs.

ACKNOWLEDGEMENT

The research is supported by the National Key Basic Research Program of China: No. 2014CB046804 and the China Ministry of Education Key Research Project "KSHIP-II Project" (Knowledge-based Ship Design Hyper-Integrated Platform): No. GKZY010004.

REFERENCES

Børhaug, E., Pavlov, A., Pettersen, K. Y. 2008. Integral LOS control for path following of underactuated marine surface vessels in the presence of constant ocean currents. *Proc. 47th IEEE Conference on Decision and Control*: 4984-4991.

Ch'ng, P. W., Doctors, L. J., Renilson, M. R.1993. A method of calculating the ship-bank interaction forces and moments in restricted water. *International Shipbuilding Progress* 40(421): 7–23.

Djouani, K. & Hamam, Y. 1995. Minimum time-energy trajectory planning for automatic ship berthing. *IEEE Journal of Oceanic Engineering* 20(1): 4-12.

Feng, P. Y., Sun, J., Ma, N. 2013. Path following of marine surface vessels using bow and aft rudders in wave fields. *Control Applications in Marine Systems* 9(1): 120-125.

Fossen, T. I., Breivik, M., Skjetne, R. 2003. Line-of-sight path following of underactuated marine craft. *Proceedings of 6th IFAC conference on manoeuvring and control of marine craft*. Girona, Spain.

Fujino, M. 1968. Studies on manoeuvrability of ships in restricted waters. *Selected Papers Journal of Society of Naval Architecture of Japan* 124: 51-72.

Lefeber, E., Pettersen, K. Y., Nijmeijer, H. 2003. Tracking control of an underactuated ship. *IEEE Transactions on Control Systems Technology* 11: 52–61.

Li, Z., Sun, J., Oh, S. 2010. Handling roll constraints for path following of marine surface vessels using coordinated rudder and propulsion control. *American Control Conference* 6010-6015.

Li, Z. & Sun, J. 2012. Disturbance compensating model predictive control with application to ship heading control. *Control Systems Technology IEEE Transactions* 20(1): 257-265.

Liu, H., Ma, N., Gu, X. C. 2016. Numerical simulation of PMM tests for a ship in close proximity to sidewall and maneuvering stability analysis. *China Ocean Engineering* 30(6):884-897.

Moreira, L, Fossen, T I, Soares, C G. 2007. Path following control system for a tanker ship model. *Ocean Engineering* 34(14-15): 2074-2085.

Mucha, P., el Moctar, O. 2013. Ship-Bank interaction of a large tanker and related control problems. *Proc. of the 32nd ASME International Conference on Ocean, Offshore and Arctic Engineering (OMAE 2013)*. Nantes, France.

Norrbin, N. H. 1974. Bank effects on a ship moving through a short dredged channel. *Proceedings of the 10th Symposium on Naval Hydrodynamics*: 71–87. Cambridge, USA.

Oh, S. R. & Sun, J. 2010. Path following of underactuated marine surface vessels using line-of-sight based model predictive control. *Ocean Engineering* 37(2):289-295.

Pettersen, K. Y. & Nijmeijer, H. 2001. Underactuated ship tracking control: Theory and experiments. *International Journal of Control* 74(14): 1435–1446.

Sano, M., Yasukawa, H., Hata, H. 2014. Directional stability of a ship in close proximity to channel wall. *Journal of Marine Science and Technology* 19(4): 376-393.

Skjetne, R., Jørgensen, U., Teel, A. R. 2011. Line-of-sight path-following along regularly parametrized curves solved as a generic maneuvering problem. *Proc. 50th IEEE Conference on Decision and Control*: 2467-2474.

Szłapczyński, R. 2013. Evolutionary sets of safe ship trajectories with speed reduction manoeuvres within traffic separation schemes. *Polish Maritime Research* 21(1): 20-27.
Thomas, B.S. & Sclavounos, P.D. 2007. Optimal control theory applied to ship maneuvering in restricted waters. *Journal of Engineering Mathematics* 58(1): 301-315.